Nano World Journal

https://doi.org/10.17756/nwj.2023-s3-120

Research Article

Open Access

Development of Advanced Nanofluids with Calcium Nitrate and Lithium Nitrate for Enhanced Thermal Energy Storage in Solar Plants

Surulivelrajan Tharmarajapandian[1*], Saritha Ganesan[2], Subramani Rajamanickam[3], Ahmed H.R. Abbas[4], I. B. Sapaev[5] and Senthil Kumar Rengasamy[6]

[1]*Department of Mechanical Engineering, Prince Shri Venkateshwara Padmavathy Engineering College, Chennai, Tamil Nadu, India*

[2]*Department of Electronics and Communication Engineering, Sairam Institute of Technology, Chennai, Tamil Nadu, India*

[3]*Department of Mathematics, Christ (Deemed to be University), Bengaluru, Karnataka, India*

[4]*College of Technical Engineering, The Islamic University, Najaf, Iraq*

[5]*Head of the department Physics and Chemistry, Tashkent Institute of Irrigation and Agricultural Mechanization Engineers, National Research University, Tashkent, Uzbekistan, Western Caspian University, Scientific researcher, Baku, Azerbaijan*

[6]*Department of Physics and Chemistry, School of Engineering, Central Asian University, Tashkent, Uzbekistan*

[7]*Department of Mathematics, AAA College of Engineering and Technology, Sivakasi, Tamil Nadu, India*

[*]Correspondence to:
Surulivelrajan Tharmarajapandian
Department of Mechanical Engineering,
Prince Shri Venkateshwara Padmavathy Engineering College,
Chennai, Tamil Nadu, India.
E-mail: surulivelt@gmail.com

Received: July 28, 2023
Accepted: October 27, 2023
Published: October 31, 2023

Citation: Tharmarajapandian S, Ganesan S, Rajamanickam S, Abbas AHR, Sapaev IB, et al. 2023. Development of Advanced Nanofluids with Calcium Nitrate and Lithium Nitrate for Enhanced Thermal Energy Storage in Solar Plants. *Nano World J* 9(S3): S657-S665.

Copyright: © 2023 Tharmarajapandian et al. This is an Open Access article distributed under the terms of the Creative Commons Attribution 4.0 International License (CCBY) (http://creativecommons.org/licenses/by/4.0/) which permits commercial use, including reproduction, adaptation, and distribution of the article provided the original author and source are credited.

Published by United Scientific Group

Abstract

This study used various approaches to create various nanofluids (NFs) by combining a molten salt mixture (60% calcium nitrate ($Ca(NO_3)_2$) - 40% lithium nitrate ($LiNO_3$)) with 2 wt.% of copper oxide (CuO)-titanium dioxide (TiO_2) nanoparticles (NPs). Concentrated solar plants can use these NFs as thermal energy storage (TES) materials by increasing the base fluid's thermal properties, which reduces the amount of storage material required. The goal of introducing new mixing processes that do not include sonication was to eliminate this stage, which could be impractical for large-scale productions, and to enable the production of a higher amount of NF. A magnetic stirrer, together with two mechanical mixers, were utilized for this specific task. A 150 g/L concentration of each NF was used to make the aqueous solution. Additionally, the most effective mixer was used to investigate the effects of different concentrations (350 and 550 g/L). To determine the specific heat, latent heat, and melting point differential scanning calorimetry (DSC) was employed. Furthermore, we measured the thermal conductivity and diffusivity of the solid-state. The specific heat increased by 32% in the solid and 16% in the liquid phase when 150 g/L was used with both mechanical mixers, according to the data. The same NFs exhibited a greater capacity to store heat as well. High solution concentrations (up to 26% and 48%, respectively) were similarly associated with an increase in thermal conductivity and diffusivity. This was particularly true for the NFs with the greatest increases in thermal properties; furthermore, they found that the best distribution of NPs was achieved at the lowest concentrations. In highly concentrated water solutions, NFs with improved thermal characteristics can be efficiently and cheaply produced utilizing mechanical mixers.

Keywords

Nanofluids, Heat transfer fluid, Molten salts, Thermal energy storage, Phase change materials

Introduction

Transporting and storing the thermal energy generated by converting solar radiation is crucial for concentrated solar power (CSP) installations [1-3]. Heat transfer fluids (HTF) are responsible for collecting heat from solar receivers and

transmitting it to either the final consumer or a suitable thermal energy storage device. The TES system's primary function is to remove heat from the HTF and reintroduce it to the HTF when the sun isn't shining. The two most common kinds of thermal storage are sensible heat (found in solids and liquids) and latent heat (found in phase change materials (PCMs)) [4, 5].

A critical component of CSP plants' ability to remain economically viable is their heat transmission and storage capabilities. The physical properties of the materials utilized (HTF and HSM) are primarily responsible for the improvement in performance and by extension, the cost-effectiveness [6, 7]. The specific heat of a material is a crucial property because it dictates the energy density (HSM), heat transfer factor, and, ultimately, the capacity of the storage system.

As a HTF and sensible heat storage medium, calcium and lithium nitrate salts are now used by several commercial CSP facilities in direct/indirect TES systems [8, 9]. Ternary salt mixes containing lithium or calcium nitrates are another example of a salt mixture that has been designed to lower the melting point and enhance the maximum operating temperature (carbonate salts). When it comes to HSMs, CSP plants that use an indirect TES system and PCMs composed of molten salts (latent heat TES) have a variety of alternatives, including hydrate, nitrate, fluoride/chloride, and carbonate salts.

Modern CSP systems frequently incorporate molten nitrate salts like HTF and HSM due to their high specific heat and density characteristics. The primary properties of the molten salts (also referred to as "solar salts"), two diathermic oils, and these other substances are compared in table 1. In medium temperature CSP plants, the volumetric heat capacity of molten salts is 38% higher than two diathermic oils, while in high temperature CSP plants, it is 52% higher. The capacity to convey heat and store heat are both noticeably enhanced as a result.

Molten salts have a high energy density, can store and release heat at a consistent temperature when employed as a PCM, and are moderately priced. But we also need to see an increase in particular heat.

In order to make PCMs (including molten salts) even more effective as HTFs or HSMs, new studies show that small amounts of NPs added to the base material can improve the material's main characteristics like thermal conductivity and specific heat. This process is called nano enhanced PCM (NEPCM) [10, 11]. Authors introduced the concept of NF; they showed that certain fluids' thermal properties might be enhanced by adding NPs of copper or aluminum. A NF is a fluid in which NPs are suspended by Brownian motion [12]. TES systems benefit greatly from improved storage media features, such as increased thermal capacity, which enables the storage of a large amount of heat in a relatively small volume. Then, at a lower cost and with the benefit of reduced energy losses (due to a reduction in the outside exchanging surfaces), compact thermal storage systems can be achieved.

According to many studies, NFs made of molten salts have an increased stored heat capacity and specific heat [13-16]. But the manufacturing process, especially the mixing procedure, determines the physical and thermal characteristics of these novel materials. The two-step process of adding NPs to a base fluid has been the most common and cost-effective way to manufacture NFs. To accomplish the dispersion of NPs in this context, sonication has frequently been employed, with subsequent water evaporation.

For large-scale industrial production of NF and NEPCM, this method is inadequate, particularly when considering the NFs' potential usage as TES media in solar power plants. To get high-quality materials at a low cost, it is necessary to choose a production process that is effective, simple, and does not consume a lot of energy. When it comes to mixing large amounts of NFs, sonication is not a practical method from an industrial standpoint. Industrial procedures are better suited to mechanical mixers. An increase in the salt and NPs concentration per liter of water can reduce the amount of water needed to produce the same volume of NF. This results in a reduction in the evaporation process, which means that less time is required to evaporate one gram of NF. Although high-temperature ovens are necessary for water evaporation, increasing the salt content strikes a balance between the two and may play a significant role in future industrialized processes.

This work aims to create new techniques for producing NFs and NEPCMs. These methods will combine salty aqueous solutions with NPs in order to produce large volumes of NFs in a single stage, all while lowering the process's total cost. We will be operating in a temperature range below 310 °C since our investigation will center on medium to high temperature applications utilizing a latent heat storage device. Data extrapolation using solar salts, including HTF and HSM, is possible even in high-temperature applications.

Materials and Method

Materials

Due to its high melting point of around 225 °C, the solar salt—a binary nitrate salt mixture of 40% $LiNO_3$ and 60% $Ca(NO_3)_2$—was selected as the principal component. The salt's liquid form is highly regarded in high temperature CSP systems for its sensible and HTF forms, as well as in medium temperature solar applications for its HSM/PCM and latent HSM forms. The second application, which can withstand

Table 1: Comparison of typical diathermic oils with the primary characteristics of molten salt.

HSM/HTF at 300 °C	Specific capacity (J/gC)	Density (kg/m³)	Volumetric capacity (kJ/m³C)	Dynamic viscosity (mPa.s)	Thermal conductivity (W/mC)
Solar salts (liquid)	1.605	1901	2842	3.31	0.61
Therminol VP1	2.424	820.0	1893	0.33	0.107
Therminol66 oil	2.679	811.6	2080	0.62	0.106

temperatures of up to 310 °C, was the primary focus of this investigation. Because of their low cost and abundance, technical grade salts were chosen on purpose for this study.

Previous research exploited these NPs and others to great effect. Researchers determined that 2 wt.% of NPs added to the basic material was the sweet spot. This percentage in the NF preparation was therefore determined to be analyzed. Table 2 shows the summary of the chosen materials' properties.

NFs synthesis procedure

The choice was made to combine the NPs and salts in a water-based solution, in keeping with previous studies, but with a reduced water volume and different laboratory mechanical mixers. As a result, NF or NEPCM could be produced at a level suitable for industrial use. For an NF solution containing NPs per liter of water and 10 g of salt, an enormous amount of water is needed, as stated in the literature.

To create the NFs used in this experiment, researchers dissolved progressively larger concentrations of salts and NPs in a 1-liter water solution. Due to the solubility of $Ca(NO_3)_2$ at 962 g/L and $LiNO_3$ at 370 g/L, we increased the concentration of the water solution to 150, 350, and 550 g/L, respectively. Because of this, we were able to produce more NF with the same amount of water. The following are the steps of the approach used to prepare the samples:

- An analytical balance with a precision of ± 62.1 mg was used to test the basic salt (BS) combination and 2 wt.% of NPs. As an example, a concentration of 150 g/L by weighting 1 g of NPs and 100 g of salts were made. The concentration of 350 g/L was achieved by weighing 300 g and 4 g, while a concentration of 550 g/L was achieved by weighing 500 g and 6 g.
- Distilled water was used to dissolve all compounds in 1 liter.
- Various technologies were used to combine salt and NP water solution.
- Once the water had evaporated, the solution was placed in an oven set at 300 °C.
- The NFs that were made were let to cool until they solidified completely.
- The powder made by grinding the solid substance was evaluated with a dry sample of a few milligrams.

The chemical was mixed using three distinct types of mixers, as previously stated.

NFs characterization

DSC analysis

The temperature and heat flow measurements taken by the calorimeter were calibrated using indium as a reference (6.4 mg). A nitrogen environment was used to heat the NFs to 300 °C for 5 min. After that, they were cooled to 150 °C at a rate of 20 °C/min. After removing any absorbed water, they were heated from 150 °C to 300 °C at a rate of 20 °C/min. In order to cancel out the sample's thermal history, guarantee excellent component mixing, and produce reproducible findings, each sample underwent four consecutive cycles in the DSC furnace without being opened. The thermal characteristics of the NFs were compared to those of the BS combination by means of the same cycle. The STARE software allows one to analyse the DSC curves and determine the following properties of the samples: melting onset temperature (T_o), end temperature (T_e), melting temperature (T_m), latent heat (ΔH), and specific heat (Cp). A conventional technique (ASTM E1269) was used for the measurements, with a 25 mg sapphire reference. When it came to the specific and latent heats, the measurement errors were 63% and 1 °C, respectively. Even though the initial cycle is known to be impacted by thermal nonequilibrium issues, it was disregarded when calculating the averages and standard deviation of the thermal parameters.

Table 2: The production of NFs requires a BS and NPs.

Material	$Ca(NO_3)_2/LiNO_3$	CuO/TiO_2
Composition (weight %)	60/40	81 - 85/13 - 17
Chemical name	Calcium nitrate/Lithium nitrate	Aerosil Cok84

Thermal conductivity and diffusivity

The thermal conductivity of the NEPCMs was examined at room temperature. The specimen made for the purpose of measuring thermal conductivity, which has a diameter of 10 °C/min and a thickness of 1 cm, is shown. Before being evaluated using a heat transfer analyzer, the samples were allowed to come down to ambient temperature. The NEPCMs on the hard materials were conducted using an appropriate surface probe that measured between 0.30 and 2 W/mK. Measurement is based on the material's response to a heat flow that is generated by an electrical heater placed near the surface of the sample. We measured thermal diffusivity (a) and thermal conductivity (k). According to the manufacturer, the thermal conductivity measurement had an accuracy of 5 - 10%. As per the requirements of ISO 8302, the manufacturer calibrated the heat transfer analyzer with reference materials that were tested using guarded hot plate apparatus.

Results

Calculating latent heat and melting point

NFs were prepared utilizing the three distinct mixers, and their melting points, heats of fusion, and temperatures at the beginning and conclusion of the melting transition were measured. The DSC curves were deemed to have peaked at the melting point. The results of the NEPCMs and the binary salt's thermal properties are displayed in table 3. All of the produced NFs exhibited an obviously increased latent heat of fusion following the addition of 2 wt.% of CuO/TiO_2 NPs to the binary salt. Improving latent heat is significant because using a material with a greater latent heat enables for more energy to be stored for the same mass of material (Figure 1).

The onset temperature remains relatively constant, while the end set temperature and melting point show a small reduction relative to the BS, with the exception of NFs produced through magnetic stirrer mixing.

Table 3: Temperatures of latent heat, melting point, NF end set, and NF onset.

NF		ΔH (J/g)	T_o (°C)	T_m (°C)	T_e (°C)
BS		115.18 ± 0.3	222.08 ± 0.2	231.88 ± 0.3	250.27 ± 0.3
1M	Magnetic stirrer 150 g/L	133.78 ± 2.3	220.68 ± 0.4	228.78 ± 0.4	254.68 ± 0.6
1D	Dispermat 150 g/L	116.27 ± 0.8	221.58 ± 0.2	227.68 ± 0.7	241.58 ± 0.5
1H	Heidolph 150 g/L	131.58 ± 1.2	220.78 ± 0.3	227.78 ± 0.3	243.98 ± 0.3
3H	Heidolph 350 g/L	121.18 ± 0.7	221.18 ± 0.4	229.28 ± 0.7	241.98 ± 0.4
5H	Heidolph 550 g/L	109.78 ± 0.4	221.68 ± 0.3	230.58 ± 0.3	245.88 ± 0.9

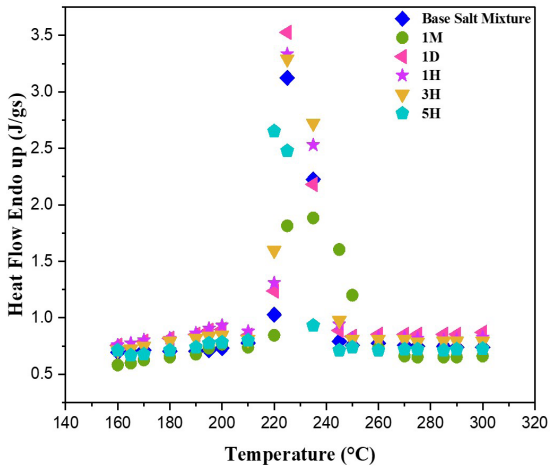


Figure 1: A variety of mechanical mixers and concentrations were used to produce heat flow curves for $Ca(NO_3)_2$-$LiNO_3$ and the NFs.

Various NFs made with water solutions containing 150 g/L and mixed using different mixers exhibited distinct behavior when compared based on these thermal parameters. A magnetic stirrer was used to combine salt and NPs in water to create the NF with the lowest onset and melting temperatures as well as the largest latent heat (139.0 J/g). The end set temperature was greater than that of the BS. The heat flow curve clearly indicates this, with 1M exhibiting a broader curve with a second peak, perhaps as a result of an inadequate mixing method.

In contrast, the end set temperature and thermal properties of the NF made using the Heidolph mixer were lower than those of the NF made using the magnetic stirrer. This prompted additional research into the NF, with a focus on the effects of varying concentrations on NFs made with the Heidolph mixer. 3H (350 g/L) and 5H (550 g/L) NFs were made.

In this situation, the latent heat and solution concentration are inversely proportional to one another, and the temperatures drop as a result. A solution concentration of 550 g/L was thus too high to ensure adequate mixing with the approach under consideration.

Out of all the NFs that have been created, 1H appears to have the highest performance due to its lower characteristic temperatures and nearly the largest latent heat. The phase-change temperature, for instance, moved down by around 4 °C and the latent heat by almost 15%.

Heat capacity

The specific heat of the nitrate mixture and the NFs produced is plotted against temperature in figure 2. The specific heat in the solid state of all of these materials is known to rise with increasing temperature, while in the liquid state, it remains constant and stable after around 260 °C. In comparison to a mixture of pure salts, the specific heat values of technical grade salts are lower. This is because the salt might contain impurities.

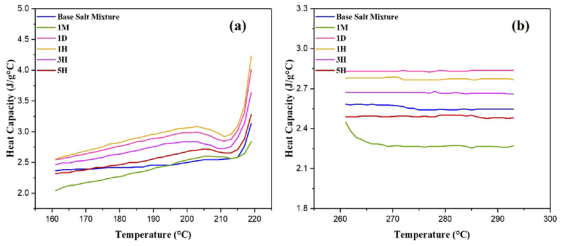


Figure 2: The specific heat of $Ca(NO_3)_2$-$LiNO_3$ and the NFs produced by various mechanical concentrations and mixers in the **(a)** solid and **(b)** liquid states as a function of temperature.

Measurements of specific temperatures in the solid phase were taken between 180 °C and 240 °C, whereas in the liquid phase they were taken between 280 °C and 320 °C. Here, 240 °C and 280 °C represent the approximate beginning and ending temperatures, respectively. All of the numbers in table 4 are averages from the thermal cycles that were examined using DSC. At least three measurements were used to calculate each value. Given that the sum of all cycles is relatively near to the value from the most recent cycle, it may be inferred that the value does not change across cycles.

NFs were made by combining 150 g of salt mixture with 1 liter of water and 1.0 wt.% of NPs exhibited variable behavior as determined by the mixer type. Using a 1M magnetic stirrer to combine the materials reduced their specific heat, especially in their solid state (8.1%). Results from using the Dispermat mixer to create a 1D NF were promising, with a specific heat rise of 29.9% in the solid state. However, the mixing process involving the Heidolph mixer (1H) resulted in the most significant improvement of this property, with an improvement of nearly 34.9% in the solid phase and 17.5% in the liquid phase.

When comparing NFs produced using the Heidolph method, it was observed that the specific heat of the NF decreased with increasing concentration of the aqueous solution. While NF 1H showed the highest specific heat increase, NF 5H had the lowest in both the solid and liquid states when compared to the BS.

Table 4: Difference between the specific heat of NFs and the BS.

Run	BS Cp (J/g°C)		Magnetic stirrer 150 Cp (J/g°C)		Dispermat 150 Cp (J/g°C)		Heidolph 150 Cp (J/g°C)		Heidolph 350 Cp (J/g°C)		Heidolph 550 Cp (J/g°C)	
	Solid	Liquid	Solid	Liquid	Solid	Liquid	Solid	Liquid	Solid	Liquid	Solid	Liquid
1	2.388	2.512	2.528	2.319	2.800	2.730	2.879	2.701	2.852	2.640	2.736	2.483
2	2.517	2.553	2.420	2.294	2.850	2.770	2.914	2.732	2.734	2.646	2.579	2.494
3	2.502	2.561	2.415	2.290	2.863	2.793	2.922	2.751	2.745	2.653	2.585	2.490
4	2.517	2.566	2.402	2.287	2.888	2.829	2.964	2.773	2.745	2.662	2.593	2.500
Mean	2.481	2.548	2.441	2.298	2.850	2.781	2.920	2.739	2.769	2.650	2.623	2.492
Std. Dev.	0.062	0.025	0.058	0.015	0.037	0.042	0.035	0.031	0.056	0.009	0.075	0.007

Solar salt's specific heat measuring capabilities were determined by testing up to 300 °C. Applications involving medium to high temperatures greatly benefit from these qualities. While solar salts have a theoretical maximum temperature tolerance of 410 °C, CSP parabolic through receivers and CSP tower receivers are limited to 570 °C and 410 °C, respectively.

Nearly everyone agrees that solar salt's specific heat follows a rule with respect to temperature at 250 °C and above [17].

$$Cp = 1{:}443 + 0{:}000172\ ^{\circ}T \quad (1)$$

Where the temperature is expressed in C and Cp is measured in J/gC.

By extending the liquid specific heat values from the experimental curves, the specific heat could be measured up to 570 °C. The particular heats that were acquired are detailed in table 5. This variance is on par with the measurement error, which is less than 5% as can be observed.

Stability of specific heat

The specific heats' stability was assessed by re-running the calorimetric experiments on the identical NFs after a year (both in liquid and solid phase). According to table 6, the specific heat of the solid phase of all of the NFs was higher than that of the fresh NFs. The largest rise of 50% was observed for 1M, which contradicts the first test findings. Even at the minimum concentration (150 g/L), the liquid phase drop that is observed in NFs generated using Heidolph and Dispermat mixers is probably within the measurement uncertainty (of about 4 %).

The specific heat of the liquid phase increased by almost 12% in NFs produced in extremely concentrated water solutions (350 and 550 g/L). Figure 3 displays the NF specific heat curves. Particularly in the solid state, the curves are shifted to lower temperatures.

The specific heats were assessed for the NFs up to 570 °C even after one year, using experimental specific heat values as an approximation. The dispersion remains below 6% even under these conditions, which is on par with the measurement error (Table 7).

Table 5: BS and NFs specific heat values extrapolated to maximum temperatures.

NFs	Factors		C = A + B x T (°C)		
	A	B (x 10^{-4})	Temp = 300	Temp = 410	Temp = 570
BS	1.7349	1.661	1.774	1.803	1.845
1M	1.5665	-3.045	1.486	1.456	1.41
1D	1.916	5129	2.058	2.11	2.189
1H	2.1097	-4.491	1.987	1.94	1.87
3H	1.9853	-4.01	1.876	1.839	1.783
5H	1.876	-5.825	1.714	1.649	1.55

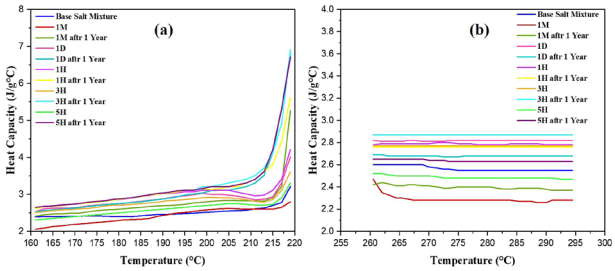


Figure 3: Various heat curves compared at 0 and 1 year after: **(a)** solid and **(b)** liquid phases.

Table 6: Specific heat NF heat compared to BS after one year.

Run	BS		Magnetic stirrer 150		Dispermat 150		Heidolph 150		Heidolph 350		Heidolph 550	
	Solid	Liquid	Solid	Liquid	Solid	Liquid	Solid	Liquid	Solid	Liquid	Solid	Liquid
1	2.388	2.512	3.002	2.267	3.372	2.709	3.370	2.694	3.353	2.787	2.933	2.633
2	2.517	2.553	3.032	2.327	3.322	2.710	3.131	2.715	3.279	2.845	2.748	2.651
3	2.502	2.561	3.049	2.361	3.316	2.707	3.135	2.718	3.283	2.837	2.750	2.653
4	2.517	2.566	3.043	2.392	3.289	2.710	3.142	2.721	3.273	2.830	2.752	2.655
Mean	2.481	2.548	3.032	2.337	3.325	2.709	3.195	2.712	3.297	2.825	2.796	2.648
Std. Dev.	0.062	0.025	0.021	0.054	0.035	0.001	0.117	0.012	0.038	0.026	0.092	0.010

Table 7: BS and NFs specific heat values extrapolated to maximum temperatures (after 1 year).

	Factors		C = a + b x T (°C)		
	A	B	Temp = 300	Temp = 410	Temp = 570
BS	1.7349	1.661 x 10^{-4}	1.7741	1.8031	1.8451
1M	2.139	-5.189 x 10^{-4}	1.9951	1.9441	1.8661
1D	2.0666	-5.189 x 10^{-4}	1.9231	1.8721	1.7941
1H	2.0294	-3.425 x 10^{-4}	1.9381	1.9051	1.8551
3H	2.1087	-2.28 x 10^{-4}	2.0511	2.0301	1.9991
5H	1.8982	-6.456 x 10^{-5}	1.8801	1.8741	1.8641

Heat storage

Additional analysis of the DSC test findings was performed, and the stored heat was evaluated in relation to the temperature. The storage capacity of each NF was determined by integrating the heat flow curves throughout the temperature range of 155 °C (minimal temperature required for solid phase) to 300 °C (highest working temperature in liquid phase).

$$Stored\ heat\left(T_{\min},T_{\max}\right)=\int_{T_{\min}}^{T_{\max}}h\left(T\right)dT \quad (2)$$

By plotting the stored heat against temperature (latent heat), one can compare the total heat that each NF stored before, during, and after the phase change (sensible heat).

As seen in figure 4, the BS combination and the produced NFs are indicated by three curves that rise above the BS curve following the phase-change temperature, indicating enhanced stored heat values. The BS had a maximum stored heat of 308.005 J/g, while the NFs' highest stored heat values for 1H, 1D, and 3H were 360.563 J/g, 351.356 J/g, and 335.667 J/g, respectively. NFs made by magnetic stirring were ineffective with regard to storage heat, in contrast to those made with 550 g/L, which exhibited comparable behavior with regard to the BS.

The Heidolph mixer also performed better than the competition when tested with a 150 g/L solution of salt and NPs in water. It is clear that the maximal stored heat of the NFs decreases with increasing concentration when comparing concentrations (150, 350, and 550 g/L) using the same mechanical mixers.

We determined the net advantage of adding NPs and utilizing different mixing techniques by analyzing the highest heat stored values for the BS and each created NF. We use equation 3 as a guide and divide the total NF heat stored by the BS to find the entire gain.

$$Total\ gain\left(\%\right)=\frac{\int_{T_{\min}}^{T_{\max}}h_{\text{mansfluid}}\left(T\right)dT}{\int_{T_{\min}}^{T_{\max}}h_{\text{PCM}}\left(T\right)dT}100 \quad (3)$$

Maximum overall gains of 15% for 1D, 18% for 1H, and 9% for 3H were achieved by NFs with improved stored heat at 300 °C, respectively. Thermal storage was not enhanced by the use of NFs 1M and 5H. These results suggest that PCMs with a higher heat capacity for storage can be produced by dissolving 150 g of salts and NPs in 1 liter of water and then mixing materials containing CuO/TiO_2 NPs with calcium and lithium nitrates in a 60:40 ratio using high-speed mechanical mixers.

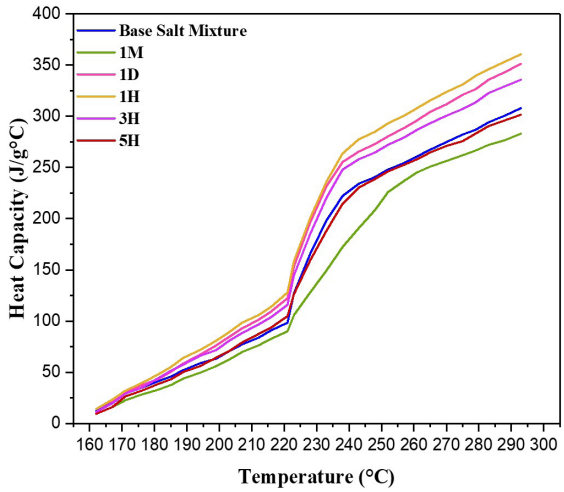


Figure 4: Heat storage vs temperature for NFs produced by various mechanical mixers and concentrations of $Ca(NO_3)_2$-$LiNO_3$ binary salt combination.

Thermal conductivity

Using the Heidolph stirrer method, the thermal conductivity of the BS and NEPCMs was measured at room temperature. The thermal conductivity value of 0.8598W/mK for the BS mixture agreed with values reported in literature [18, 19], as shown in table 8. The thermal conductivity rose as the concentration of the aqueous solution grew (from 150 to 550 g/L), and the NFs show greater values compared to the BS mixture. At 350 g/L and 550 g/L concentrations, the conductivity of the NFs is 21.8% and 27.0% greater than that of the calcium-lithium nitrate mixture, respectively; at the same concentrations, the thermal diffusivity is roughly 12% and 48% higher. NF 1H has reduced thermal conductivity and diffusivity in this case.

Discussion

In this study, three distinct mixing procedures were executed. The mixing process, the capacity to mix a large volume of solution, and the energy supplied during mixing were all factors in their selection. Due to the stirrer's inability to create extremely high shear mixing into the water solution, magnetic stirring, the initial technique, likely did not yield satisfactory outcomes. The resultant NF lacked improved thermal characteristics and NPs dispersion, even after using the largest stirrer at the highest speed setting. The magnetic stirring approach was found to significantly induce aggregation when NPs are

Table 8: Heidolph mixer-produced NFs and the BS's thermal conductivity and diffusivity.

NFs	k (W/m K)	inc. %	a (10^6 m^2/s)	inc. %
BS	0.8598 ± 0.015	-	0.5338 ± 0.011	-
1H	0.6338 ± 0.013	- 35.8	0.4178 ± 0.008	- 33.3
3H	0.9327 ± 0.012	24.8	0.5758 ± 0.007	15.4
5H	0.9856 ± 0.014	30	0.7298 ± 0.009	52.7

synthesized [20-22]. The dispersion of NPs in a water-salt mix could potentially lead to the same result.

Applying the standard coagulation theory of colloids to the aggregation caused by magnetic stirring provides a possible explanation. Stirring has the ability to achieve two opposing effects: first, it can disperse particles in a liquid and break up aggregates, and second, it can promote colloidal coagulation by increasing the intensity and likelihood of particle collisions through shear mixing.

Mechanical shaft rotation, on the other hand, appears to produce higher shear mixing, which improves the NFs' thermal characteristics. The results of the second and third rounds of mixing were these. The speed and kind of impeller employed are the primary differentiating factors between them. Providing high shear mixing, the Dispermat dissolver did its job. A dissolver disc, which is ideal for working with NFs and other low-viscosity liquids, was employed as the stirring instrument. It had a dispersion impeller with a diameter of 40 mm and could reach mixing speeds of up to 20,000 rpm. To produce NPs dispersion in a salt and water mixture, the Dispermat method employs a rotating dissolver disc at the shaft's tip to create efficient mixture circulation. Consequently, the Dispermat's dispersion is a product of the unique geometry of the spinning disc. The agglomerations that settle inside the zones of low and high pressure caused by the disk's fast motion through the fluid are rapidly dispersed because the agglomerations are subjected to alternate stress. Furthermore, the agglomerates are destroyed by the impact they experience when they reach the surface and the margins of the fins.

The surfaces of the disc, however, do a disproportionate amount of dispersion work. The blade's fast motion causes shear stress on the upper and lower surfaces, which initiates the dispersion process. The disc's bottom surface to vessel bottom distance is a key parameter that governs the disc-to-vessel shear stress.

The size of the agglomerates decreased as the shear mixing intensity increased and the concentration of the aqueous solution decreased, in accordance with the dispersion effects of the various mixing methods.

The larger impeller and the speed utilized during mixing may explain why NF 1H had better NPs distribution compared to 1M and 1D, as well as the greater improvement in thermal characteristics.

Two major phases were required for the NPs to disperse in the water-salt mixture: wetting and deagglomeration. In order to accomplish efficient wetting, a portion of the water was mixed with NPs and nitrate salts, creating a solid-liquid contact instead of a solid-air one. After that, the NF was able to de-agglomerate thanks to the mechanical stirrers. It appears that the energy required to shatter the nanomaterial agglomerates was supplied by the overhead stirrer impeller.

Additionally, it appears that the NPs are better dispersed at the low solution concentration of 150 g/L. Actually, more agglomerated NPs were found in NFs 3H and 5H according to the morphological investigation. While the existence of dispersed NPs is required for an increase in specific heat, the lowest rise in thermal conductivity in NF 1H is believed to be due to NPs agglomeration into clusters. Although these parameters were found to be reduced for NF 1H when tested thermally alone, DSC data confirmed that specific heat was higher for NF 1H compared to 3H and 5H.

That the maximum stored heat drops with increasing particle concentration makes sense when remember that the stored heat is the sum of the sensible and latent heats that a material has (as shown in equation 2). As a result, the paths of heat movement are connected. The diagrams make it quite evident that the total stored heat is equal to the sum of the practical temperatures of the NFs 1H, 3H, and 5H. Hence, the variation in latent heat is mostly responsible for the drop in stored heat with increasing concentration. The data showing that the NFs' enthalpies decrease with increasing concentration (150, 350, and 550 g/L) is presented in table 4.

It is also possible to compare the outcomes of this study to those of other dispersion strategies. Multiple investigations have shown that a two-step liquid solution followed by sonication is the most typical strategy. One of these utilized the same salt mixture that was investigated in our study to make a NF. When using NPs of CuO of 5, 10, 30, and 60 nm in size, a concentration of 2% by weight was consistently exhibited. However, these improvements are lower than the values that we achieved.

In contrast, NFs containing TiO_2 NPs and the same solar salt that was examined here showed a general decline in specific heats using a two-step liquid solution technique and sonication. Nevertheless, the drop is likely caused by the excessive number of NPs that were used (varying between 0.9% and 4.6% by volume, which equates to weight fractions greater than 1% when taking into account the highest weight fraction capable of enhancing thermal characteristics).

To further examine the NFs generated here with and without sonication, one can use an ultrasonicator to combine the same NPs (i.e., with 1.0 wt.% of CuO/TiO_2) with BS in a 10 g/L water solution. When comparing NFs made in low-concentration solutions using an ultrasonicator (+57.7% in solid form + 22.5% in liquid form) to those made in high-concentration solutions using mechanical mixing, it is clear that the latter produced lower specific heat improvements.

Further improvements to the already high-quality outcomes could be made by adjusting the mixing settings, such as the mixing time (with 31% in solid form and 14% in liquid form, respectively).

The eutectic nitrate mixtures studied in this work also had TiO_2 and CuO NPs dispersed into them using the dry milling process. Even with a small number of NPs (0.2 - 0.6 wt.%), there were noticeable gains in specific heat. Specific heat increased by 2.9% with 1.2 wt.% CuO NPs and 3.1% with TiO_2 NPs when tested at 300 °C. Our aim was to test the specific heat values of NFs at 300 °C and compare them to these results; we found an increase of 19.4% for 1D, 13.4% for 1H, and 5.8% for 3H. Therefore, it is reasonable to assume that the NPs and dispersion method employed in our work played a role in the elevated specific heat.

NFs' thermal characteristics have recently been enhanced using a novel high-temperature dispersion approach, which allows for direct liquid-state processing. Here, a twin-screw micro-compounder was used to mix several NPs (including the CuO/TiO_2 mix employed in our work) with $Ca(NO_3)_2$-$LiNO_3$ (60 - 40 wt.%) at 300 °C. The solid phase specific heat increase for this NF was 52.3% higher than the Heidolph mixer values, whereas the liquid phase specific heat improvement was 20.0% similar.

A small shift toward lower temperatures in the heat flow curves, particularly in the solid phase, is the usual explanation for an increase in specific heat. A larger portion of the melting phase and the majority of the curves fall within the temperature range of 180 - 240 °C, which is also the region in which the specific heats were computed for the NFs at time zero. Therefore, the temperature range for NFs has a larger melting contribution after one year compared to zero. The NPs likely function as impurities, causing the melting to begin at lower temperatures than when the NFs are fresh.

After a year, there is a little shift toward lower temperatures in the heat flow curves, particularly in the solid phase, which could explain the specific heat rise. With NPs as impurities, the melting point is likely to be lower than fresh NFs. The melting contribution for NFs after one year is more than it was at time zero since their specific temperatures were computed within the same temperature from (180 °C to 240 °C). In this region of the phase change curves, the computed specific heat values increased.

NPs have several beneficial effects, one of which is lowering melting points. This is particularly true when the Heidolph mixing method is employed to transmit heat in parabolic via plants using solar salts. In reality, mixes with lower melting points are necessary for solar applications in order to facilitate the operation of the solar field and prevent salt from freezing.

There is a lack of obvious justification for the increase in latent heat, and very few articles record or explain its variance. NFs composed of the same solar salt ($Ca(NO_3)_2$-$LiNO_3$) and pure lithium nitrate combined by ultrasonication showed comparable improvements. The latent temperatures of $Ca(NO_3)_2$-$LiNO_3$ and pure lithium nitrate were both increased by 16% and 12%, respectively, when 2 wt.% of CuO/TiO_2 NPs were added.

Still, a 4.9% rise in latent heat was shown when the identical NPs and BS were combined directly in a liquid form at 320 °C, without the need for water or sonication. In this instance, it was thought to be because the NPs caused the salt to crystallize more. The amount of energy (and hence latent heat) required to undergo a structural change from an ordered (i.e., crystalline) state is directly proportional to this change.

Low latent heat enhancements (+2.6% and +4.0% with CuO and TiO_2 NPs) were observed even in NFs derived from the identical eutectic mixture of calcium and lithium nitrate as those utilized in our work, which was prepared using dry milling. These results were also attained by dispersing minute quantities of NPs (0.2 wt.% CuO and 0.6 wt.% TiO_2), while larger percentages approaching 1.2 or 1.6 wt.% were used to decrease the latent heat. Because the NF contained nanostructures, the authors concluded that this was the cause of the enthalpy increase. The NFs with smaller aggregates exhibited the highest latent heat increase, our results suggest that this may be because of differences in mixing procedures (they employed a dry milling approach).

It is reasonable to assume that the NFs' layer of tiny agglomerates is responsible for the improvement, as it would trap the NPs. Therefore, the latent heat would increase since more energy would be required to melt the solid trapped in these clusters. Additional bonding between NPs and water molecules, the base fluid, may be the reason for the rise in latent heat in NFs. Thus, an increase in latent heat is induced during phase change because more energy is needed to break the additional bonds. Additional research is required to determine the causes of the rise in the heat of fusion.

Conclusion

NFs containing NPs manufactured on a massive scale and a binary nitrate salt mixture (60 wt.% $Ca(NO_3)_2$ and 40 wt.% $LiNO_3$) are the subject of this thermal characterization investigation. High temperature solar concentrated plants can make use of these NFs as HTF and HSM. NFs with varying thermal properties were created by employing various mixing techniques. The thermal characteristics of NFs and the varied agglomeration sizes were both affected by the mixing procedure. It was found that magnetic stirring was not as effective as high shear mixing in dispersing the NPs. This led to an increase in thermal conductivity and a decrease in specific heat. Also, when the salts and NPs were mixed with water at the minimum concentration (150 g/L), the NFs showed an improvement in NPs distribution and an enhancement of thermal properties. Synthesized NFs with specific heat gains and thermal conductivity increases as high as 350 g/L in water solutions may find use in TES. The primary outcomes of NEPCM production are NFs with low melting points, high specific heats, and excellent thermal conductivity and stored heats. Both heat transmission and TES rely on these characteristics. This study showed that it is possible to mass-produce NFs with better thermal properties in solutions with small to medium volumes of water utilizing an overhanging mixer with the largest impeller.

Acknowledgements

None.

Conflict of Interest

None.

References

1. Prasad AR, Kumar SKD, Banu TV, Vignesh T, Aatthisugan I. 2019. Synthesis and thermal energy storage analysis of copper oxide nano fluid for heat transfer applications. *Int J Innov Technol Explor Eng* 8(11): 3616-3619.
2. Basit MA, Farooq U, Imran M, Fatima N, Alhushaybari A, et al. 2023. Comprehensive investigations of (Au-Ag/Blood and Cu-Fe_3O_4/blood) hybrid nanofluid over two rotating disks: numerical and computational approach. *Alexandria Eng J* 72: 19-36. https://doi.org/10.1016/j.aej.2023.03.077

3. Agrawal R, Singh KDP, Paswan MK. 2020. Review on enhancement of thermal conductivity of phase change materials with nano-particle in engineering applications. *Mater Today Proc* 22: 1617-1627. https://doi.org/10.1016/j.matpr.2020.02.159
4. Jahromi MSB, Kalantar V, Akhijahani HS, Kargarsharifabad H. 2022. Recent progress on solar cabinet dryers for agricultural products equipped with energy storage using phase change materials. *J Energy Storage* 51: 104434. https://doi.org/10.1016/j.est.2022.104434
5. El-Sayed WG, Attia NF, Ismail I, El-Khayat M, Nogami M, et al. 2021. Innovative and cost-effective nanodiamond based molten salt nanocomposite as efficient heat transfer fluid and thermal energy storage media. *Renew Energy* 177: 596-602. https://doi.org/10.1016/j.renene.2021.05.135
6. Shafee SM, Gnanasekaran K, Solomon GR, Balaji R. 2020. Preparation and analysis of novel paraffin based stable nano fluid dispersed with carbon nano tubes as effective phase change material for free cooling applications. *Mater Today Proc* 33: 4526-4532. https://doi.org/10.1016/j.matpr.2020.08.054
7. Agarwal A, Molwane OB, Pitso I. 2021. Thermal analysis & modelling of phase change material used in low temperature industrial wastewater applications. *Mater Today Proc* 39: 596-605. https://doi.org/10.1016/j.matpr.2020.08.612
8. Kushwaha PK, Sharma NK, Kumar A, Meena CS. 2022. Recent advancements in augmentation of solar water heaters using nanocomposites with PCM: past, present, and future. *Buildings* 13(1): 79. https://doi.org/10.3390/buildings13010079
9. Lovera-Copa JA, Ushak S, Reinaga N, Villalobos I, Martínez FR. 2020. Design of phase change materials based on salt hydrates for thermal energy storage in a range of 4-40 °C. *J Therm Anal Calorim* 139: 3701-3710. https://doi.org/10.1007/s10973-019-08655-1
10. Wei X, Zhang X, Ding J, Wang W, Lu J. 2019. The effect of nano-MgO on thermal properties of ternary chloride fluid. *Energy Procedia* 158: 773-778. https://doi.org/10.1016/j.egypro.2019.01.205
11. Fan YY, Lin RH, Yang H, Huang CM, Liu Y, et al. 2020. Effects of different salts on the structure of cassava starch. *Food Fermentation Ind* 46(3): 84-89. https://doi.org/10.13995/j.cnki.11-1802/ts.022256
12. Zhang X, Lu Y, Yu Q, Wu Y, Zhang C. 2021. Study on preparation and thermophysical characteristics of molten salt nanocomposite by microwave method. *Sol Energy Mater Sol Cells* 220: 110846. https://doi.org/10.1016/j.solmat.2020.110846
13. Marcos MA, Podolsky NE, Cabaleiro D, Lugo L, Zakharov AO, et al. 2019. MWCNT in PEG-400 nanofluids for thermal applications: a chemical, physical and thermal approach. *J Mol Liq* 294: 111616. https://doi.org/10.1016/j.molliq.2019.111616
14. Liu H, Yang J, Zheng H, Chen Y, Li Y. 2021. Investigation on the micromorphology and thermophysical properties of $NaNO_3$ heat storage materials modified by solution combustion. *Micron* 148: 103103. https://doi.org/10.1016/j.micron.2021.103103
15. Cui L, Yu Q, Huang C, Zhang Y, Wang Y, et al. 2023. Nanoadditives induced enhancement of thermal energy storage properties of molten salt: insights from experiments and molecular dynamics simulations. *J Energy Storage* 72: 108612. https://doi.org/10.1016/j.est.2023.108612
16. Han Z, Ram MK, Kamal R, Alamro T, Goswami DY, et al. 2019. Characterization of molten salt doped with different size nanoparticles of Al_2O_3. *Int J Energy Res* 43(8): 3732-3745. https://doi.org/10.1002/er.4531
17. Kang Z, Huang S, Liu X, Zhang Y, He M. 2023. A novel high temperature eutectic salt and its composite with enhanced high conductivity. *J Energy Storage* 59: 106409. https://doi.org/10.1016/j.est.2022.106409
18. Prado JI, Vallejo JP, Lugo L. 2022. A new relationship on transport properties of nanofluids. Evidence with novel magnesium oxide based n-tetradecane nanodispersions. *Powder Technol* 397: 117082. https://doi.org/10.1016/j.powtec.2021.117082
19. Aljaerani HA, Samykano M, Pandey AK, Kadirgama K, Saidur R. 2020. Thermo-physical properties and corrosivity improvement of molten salts by use of nanoparticles for concentrated solar power applications: a critical review. *J Mol Liq* 314: 113807. https://doi.org/10.1016/j.molliq.2020.113807
20. Selvaraj V, Morri B, Nair LM, Krishnan H. 2019. Experimental investigation on the thermophysical properties of beryllium oxide-based nanofluid and nano-enhanced phase change material. *J Therm Anal Calorim* 137: 1527-1536. https://doi.org/10.1007/s10973-019-08042-w
21. Zhou W, Yang Z, Feng Y, Lin L. 2022. Insights into the thermophysical properties and heat conduction enhancement of NaCl-Al_2O_3 composite phase change material by molecular dynamics simulation. *Int J Heat Mass Transf* 198: 123422. https://doi.org/10.1016/j.ijheatmasstransfer.2022.123422
22. Lu J, Zhang Z, Wang W, Ding J. 2021. Effects of MgO nanoparticles on thermo-physical properties of $LiNO_3$-$NaNO_3$-KNO_3 for thermal energy storage. *Energies* 14(3): 677. https://doi.org/10.3390/en14030677